JASA ARTICLE

# Shear waves and sound attenuation in underwater waveguides

Oleg A. Godin[a)]
*Department of Physics, Naval Postgraduate School, 833 Dyer Road, Monterey, California 93943-5216, USA*

**ABSTRACT:**
In addition to dissipation of acoustic energy in the seabed, bottom-interacting normal modes are attenuated by radiation of shear waves into soft sediments, where shear speed is small compared to the sound speed in water. The shear-wave contribution and the dissipation have distinct frequency dependencies, and their relative magnitude affects the observed frequency dependence of mode attenuation. Previous studies suggested that the shear-wave contribution to the attenuation is proportional to the cube of the small ratio of the shear and sound speeds. Here, coupling of compressional and shear waves in layered soft sediments is analyzed. Besides the well-known, third-order contribution to the attenuation due to shear-wave generation at the water-sediment interface, a stronger, first-order, contribution is found to occur due to compressional-to-shear wave conversion at interfaces within the sediment. First-order effects of weak shear on mode travel times are also identified. Stratification of the sediment density and interference of shear waves reflected within the seabed control the frequency dependence of the shear-wave contribution to sound attenuation. With the shear-wave contribution being larger than previously estimated, its effect on the experimentally measured frequency dependence of the sound dissipation may need to be re-assessed.
https://doi.org/10.1121/10.0004999
(Received 2 March 2021; revised 20 April 2021; accepted 21 April 2021; published online 26 May 2021)
[Editor: Nicholas P. Chotiros] Pages: 3586–3598

## I. INTRODUCTION

Coupling to shear waves in solids or viscous (vorticity) waves in fluids is a well-known mechanism of energy loss (attenuation) of compressional waves.[1–3] Unlike the intrinsic absorption (conversion of mechanical energy to heat), the coupling occurs only in inhomogeneous or bounded solids and viscous fluids. In underwater waveguides, shear-wave contributions to sound attenuation[4,5] are most significant for bottom-interacting normal modes that propagate over a seabed, where shear speed is less than the phase speed of the mode. In propagating normal modes, compressional waves become evanescent in the seabed and carry acoustic energy horizontally as long as dissipation is negligible. In contrast, shear waves are not evanescent and transport energy deep into the seabed. In the absence of dissipation, coupling to shear waves is the only mechanism of exponential attenuation of propagating normal modes in range-independent waveguides.

The shear-wave speed is much smaller than the compressional wave speed and the sound speed in water in many types of marine sediments,[4,6] while the evanescent compressional wave field in propagating modes is often negligible deep in the seabed, where the shear speed is large. Under these conditions, the seabed is typically described as a stratified fluid in the sound propagation modeling,[5,7] with the shear-wave effects presumably included via "effective" values of the sound speed, the density, and the attenuation coefficient of compressional waves in the fluid bottom.

Understanding and accurate evaluation of the shear-wave contributions to sound attenuation are necessary for modeling and interpretation of the sound transmission loss in shallow-water waveguides and for sonar performance predictions from low to mid-frequencies.[5,8] Quantifying the shear-wave contributions to attenuation of normal modes is important for modeling and interpretation of the power spectra, modal content, and vertical directionality of low-frequency ambient sound in shallow water[9–13] as well as in applications of noise interferometry to passive remote sensing of the coastal ocean.[14,15] An accurate prediction of the shear-wave contribution to sound attenuation at different frequencies is required[8,16,17] to interpret the empirical models of the linear[4,6] and power-law with a fractional exponent $\kappa$, $1.6 < \kappa < 2$,[18,19] frequency dependencies of the attenuation and evaluate applicability[17,20] of the physics-based models of wave propagation in the porous seabed, such as Biot theory and its extensions[21–24] and Buckingham's viscous grain shearing theory.[25,26]

Shear-wave contributions to sound attenuation in the seabed have been studied theoretically with the bottom modeled as a homogeneous solid half-space.[5,16,27,28] When the shear speed $c_t$ is small compared to the compressional wave speed $c_l$, the sound attenuation due to conversion to shear waves was found to be proportional to the third power of the small parameter $c_t/c_l$. Corrections to the phase and group speeds of the normal modes were found to be of the second order in $c_t/c_l$.[16,27,29] Pierce and Carey[17] and Carey *et al.*[8] argued that the same cubic dependence of the attenuation on $c_t$ extends to the stratified seabed. The standard perturbation theory for normal modes in solid and fluid-solid

[a)]Electronic mail: oagodin@nps.edu, ORCID: 0000-0003-4599-2149.

https://doi.org/10.1121/10.0004999

waveguides[30–32] also suggests that weak shear rigidity of the bottom changes the normal mode wavenumbers by quantities of the second and higher orders in the shear-wave speed $c_t$.

The analyses in Refs. 5, 8, 16, 17, and 27 account for the shear-wave generation at the water-sediment interface but overlook the strongest contribution to the compressional-to-shear wave conversion, which occurs *within* the stratified seabed, e.g., at interfaces between sediment layers of distinct composition. In this paper, the effect of weak shear rigidity on dispersion of acoustic normal modes and the shear-wave contributions to sound attenuation are studied using a simple model of the seabed as a viscoelastic solid layer overlying a viscoelastic half-space. No restrictions are imposed on the water column properties other than the waveguide being range independent. It is demonstrated that coupling between compressional and shear waves in the bottom with density stratification results in significant, first-order contributions to sound attenuation and first-order changes in the normal mode dispersion.

The remainder of the paper is organized as follows. An explicit expression is derived in Sec. II A for the mode wavenumber perturbations in terms of the bottom impedance perturbations due to variations in the physical properties of the seabed. Thus, the problem of characterizing the effects of weak shear rigidity on mode dispersion and attenuation in an arbitrary range-independent waveguide is reduced to calculation of the acoustic impedance of the bottom. Coupling of plane compressional and shear waves at solid-solid and fluid-solid interfaces is discussed in Sec. II B, and simple equations are obtained for the reflection, transmission, and transformation coefficients at interfaces involving soft solids. Leading-order asymptotic contributions of weak shear rigidity to the input impedance of two-layered seabed are derived analytically in Sec. II C. Using symbolic computations, a compact expression for the effect of weak shear rigidity is obtained from the algebraically complex exact equation for the impedance of a stratified solid bottom. Theoretical results of Sec. II are illustrated in Sec. III for several geoacoustic models, including calculation of the apparent sound attenuation caused by the coupling between compressional and shear waves in a stratified seabed with small shear speed. Section IV points out the limitations of the standard perturbation theory for modes in solid waveguides[30–32] when applied to stratified soft solids. Implications of our theoretical results for measurements of sound attenuation and the frequency dependence of the intrinsic compressional wave dissipation in soft marine sediments are also discussed in Sec. IV. Section V summarizes our findings.

## II. THEORY

We consider sound propagation in a range-independent underwater waveguide with an arbitrarily stratified water column and a seabed composed of a homogeneous sediment layer overlying a homogeneous half-space (sub-bottom). The seabed will be modeled as either a fluid or an isotropic (viscoelastic) solid. Introduce a Cartesian coordinate system $(x, y, z)$ with the vertical coordinate z increasing downward. $x$-, $y$-, and $z$-components of the particle displacement vector $\mathbf{u} = (u_1, u_2, u_3)$ and other vectors will be denoted by subscripts 1, 2, 3. A pressure-release ocean surface is located at $z = -H$, the seafloor is at $z = 0$, and the interface between the sediment layer and sub-bottom is at $z = h$ [Fig. 1(a)]. Acoustic properties of the seabed as sensed by a normal mode will be characterized by impedance of the seafloor defined as the ratio of acoustic pressure to the vertical component of particle velocity at $z = 0$ in the normal mode.

### A. Perturbation of normal modes by a change in the seafloor impedance

Changes in the physical parameters of the seabed lead to variations in the phase speed and/or attenuation of the bottom-interacting normal modes. Here, we derive a simple quantitative relation between small variations, or perturbations, of the normal mode wave number and acoustic impedance of the seabed in a generic range-independent waveguide.

The vertical dependence of the acoustic pressure $p_j$ in a monochromatic normal mode satisfies the one-dimensional reduced wave equation[3,33]

$$\frac{\partial}{\partial z}\left(\frac{1}{\rho_w}\frac{\partial p_j}{\partial z}\right) + \left(\frac{\omega^2}{c_w^2} - \xi_j^2\right)\frac{p_j}{\rho} = 0, \tag{1}$$

where $\omega$ and $\xi_j$ are the wave frequency and the mode wave number, and $c_w(z)$ and $\rho_w(z)$ are the sound speed and density profiles in the water column. The index $j = 1, 2$ distinguishes acoustic fields in two waveguides with different seabed properties. At the sea surface $p_j(-H) = 0$. At the seafloor $z = 0$ the acoustic pressure satisfies the boundary condition

$$Z_j(\omega, \xi_j)\frac{\partial p_j}{\partial z} - i\omega\rho_w p_j = 0, \quad z = -0, \tag{2}$$

where $Z_j$ is the acoustic impedance of the seabed. Arbitrary fluid or solid horizontally stratified seabed can be characterized by the appropriate dependence of its input acoustic impedance on wave frequency and the horizontal wave number $\xi_j$. In Eq. (2) and below, $z = -z_0$ and $z = +z_0$ denote, respectively, points just above and just below the horizontal interface $z = z_0$.

We want to compare the wave numbers $\xi_j$, $j = 1, 2$, of the normal modes of the same order that propagate in two range-independent waveguides, which share the same water column properties but have different bottoms and, hence, distinct impedances $Z_1(\omega, \xi)$ and $Z_2(\omega, \xi)$. By subtracting the product of $p_2$ and Eq. (1) with $j = 1$ from the product of $p_1$ and Eq. (1) with $j = 2$, one obtains

$$\frac{\partial}{\partial z}\left(\frac{p_1}{\rho_w}\frac{\partial p_2}{\partial z} - \frac{p_2}{\rho_w}\frac{\partial p_1}{\partial z}\right) = \left(\xi_2^2 - \xi_1^2\right)\frac{p_1 p_2}{\rho_w}. \tag{3}$$

Integrating Eq. (3) over depth and taking into account the boundary conditions at the ocean surface and bottom, Eq. (2), gives

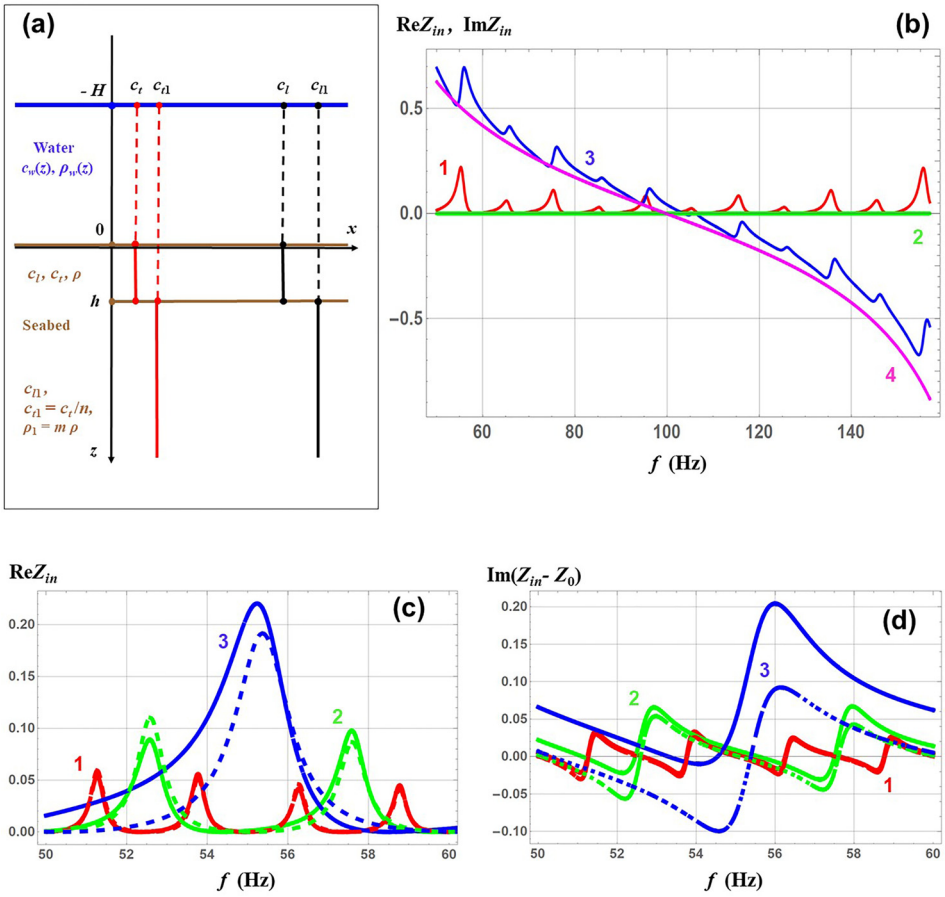


FIG. 1. (Color online) Acoustic impedance of soft solid seabed. (a) Geometry of the problem. (b) Comparison of the frequency dependences of the normalized impedance of fluid bottom (lines 2 and 4) and solid bottom with the shear speed $c_t = 200$ m/s in the top sediment layer (lines 1 and 3). The real and imaginary parts of the impedance are shown by lines 1 and 2 and lines 3 and 4, respectively. (c) The fine structure of the frequency dependence of the real part of the normalized impedance of the solid seabed is shown in a narrow frequency band for three values of the shear speed in the top sediment layer: $c_t = 50$ m/s (1), 100 m/s (2), and 200 m/s (3). The exact and first-order approximate results are depicted by solid and dashed lines, respectively. (d) Same as (c) but for the imaginary part of the difference between the impedances of solid and fluid bottoms. In (b)–(d), the layer thickness $h = 10$ m. The ratio of densities in the half-space and in the layer is $m = 2$; the ratio of shear speeds in the layer and the half-space is $n = 0.5$. Compressional wave speeds are $c_l = 1500$ m/s in the layer and $c_{l1} = 1900$ m/s in the half-space. Normal mode phase speed is 1700 m/s. Impedances are normalized by the absolute value of the frequency-independent impedance of the fluid half-space with compressional speed and density of the half-space $z > h$.

$$i\omega p_1(-0)p_2(-0)\left[\frac{1}{Z_2(\omega,\xi_2)}-\frac{1}{Z_1(\omega,\xi_1)}\right] = (\xi_2^2-\xi_1^2)\int_{-H}^{0}\frac{dz}{\rho_w}p_1p_2. \tag{4}$$

No approximations have been made in derivation of Eq. (4).

When $Z_1$ represents an unperturbed seabed, and small variations of its parameters change the bottom impedance to $Z_2 = Z_1(\omega, \xi) + \delta Z(\omega, \xi)$ and the mode wave number from $\xi_1$ to $\xi_2 = \xi_1(\omega) + \delta\xi(\omega)$, the perturbations $\delta Z/Z$ and $\delta\xi$ are small; $p_2 \to p_1$ in the limit $\delta Z \to 0$. Linearization of Eq. (4) with respect to small perturbations of the acoustic pressure, bottom impedance, and mode wave number gives

$$\delta\xi = -\frac{i\omega\delta Z}{Z_1^2}\Big/\left[\frac{2\xi_1}{p_1^2(-0)}\int_{-H}^{0}\frac{dz}{\rho_w}p_1^2+\frac{i\omega}{Z_1^2}\frac{\partial Z}{\partial\xi}\right]\Bigg|_{\xi=\xi_1}. \tag{5}$$

Alternatively, one can write Eq. (4) in terms of the input acoustic admittances, $Y_j = 1/Z_j$, $j = 1, 2$, of the seabed. When the admittance difference $\delta Y = Y_2 - Y_1$ is small, linearization of Eq. (4) with respect to perturbations gives

$$\delta\xi = i\omega\delta Y\Big/\left[\frac{2\xi_1}{p_1^2(-0)}\int_{-H}^{0}\frac{dz}{\rho_w}p_1^2-i\omega\frac{\partial Y_1}{\partial\xi}\right]\Bigg|_{\xi=\xi_1}. \tag{6}$$

The right-hand sides in Eqs. (5) and (6) are evaluated at the unperturbed value $\xi = \xi_1$ of the modal wavenumber. Note that knowledge of only the acoustic field in the unperturbed waveguide is needed to calculate the mode wavenumber perturbation with Eq. (5) or (6). The impedance may equal zero [e.g., at a pressure-release surface; see also Fig. 1(b)] or become infinite (e.g., at a rigid surface or at mode cutoff frequencies in a Pekeris waveguide). Equations (5) and (6) are generally equivalent, but Eq. (6) is more convenient in the vicinity of singularities of $Z_1(\omega, \xi)$, and Eq. (5) is more convenient in the vicinity of nulls of $Z_1(\omega, \xi)$. Following the derivation of the normal mode perturbation theory in Refs. 33 and 34, one can readily extend the result given by

https://doi.org/10.1121/10.0004999

Eqs. (5) and (6) to waveguides in moving fluids and to acoustic-gravity waves. These extensions are not required, though, for the purposes of this paper.

For the same unperturbed seabed structure and its perturbations, different perturbations in the modal phase speed and attenuation occur, depending on the water depth and the sound speed profile in water. By using the input impedance $Z$ or admittance $Y$ to characterize the seafloor and calculating modal perturbations from Eqs. (5) and (6), one can isolate the effects of the water column and seabed effects.

In the absence of dissipation, the mode wave number $\xi_1$ and normalized mode shape function $p_1(z)/p_1(-0)$ are real-valued in propagating (as opposed to evanescent) normal modes.[33] It follows from the impedance definition Eq. (2) that acoustic impedance of the seabed is purely imaginary for propagating normal modes. When Eqs. (5) and (6) are used to describe a perturbation of a propagating normal mode, $\mathrm{Im}\delta Z$ and $\mathrm{Im}\delta Y$ contribute to the real part of the perturbed mode wave number and, hence, are responsible for the mode phase speed perturbation. Real parts of $\delta Z$ and $\delta Y$ are responsible for $\mathrm{Im}\delta\xi$ and, thus, contribute to mode attenuation.

In the particular case of a waveguide with the bottom impedance $Z_b(\omega, \xi)$ and constant sound speed $c_w$ and density $\rho_w$ in water, modal wavenumbers $\xi$ can be found by solving the explicit dispersion equation[35]

$$\omega\rho_w \tan(\alpha_w H) = i\alpha_w Z_b, \tag{7}$$

where $\alpha_w = \sqrt{\omega^2 c_w^{-2} - \xi^2}$. Because of the boundary conditions at the pressure-release boundary $z = -H$, the vertical variation of acoustic pressure in the normal mode is

$$p(\xi, z) = p(\xi, -0)\sin(\alpha_w z + \alpha_w H)/\sin\alpha_w H, \quad -H < z < 0. \tag{8}$$

The mode wavenumber $\xi$, which satisfies the dispersion equation (7), depends on the impedance $Z_b$. Let $\xi_1$ and $\xi_1 + \delta\xi$ satisfy Eq. (7) with $Z_b = Z_1(\omega, \xi)$ and $Z_b = Z_1(\omega, \xi) + \delta Z(\omega, \xi)$, respectively. Then, by differentiating both sides of Eq. (7) with respect to $\xi$, we find

$$\delta\xi = -\frac{i\omega\delta Z}{Z_1^2} \Bigg/ \left[\frac{\xi_1(2\alpha_w H - \sin 2\alpha_w H)}{2\alpha_w\rho_w \sin^2\alpha_w H} + \frac{i\omega}{Z_1^2}\frac{\partial Z}{\partial\xi}\right]\Bigg|_{\xi=\xi_1} \tag{9}$$

to first order in $\delta Z$. Using Eq. (8), it is straightforward to verify that the general Eq. (5) agrees with the explicit result (9) in this particular case.

Below, we focus on characterizing the difference $\delta Z$ between the acoustic impedances of a fluid bottom and a solid seabed with weak shear rigidity. The impedance change is caused by coupling of the shear and compressional waves.

### B. Conversion between compressional and shear waves at an interface

This paper considers sound propagation over a seabed, where top layers are "soft," i.e., the shear-wave speed $c_t$ is small compared to compressional wave speed $c_l$. For brevity, these speeds will be referred to as shear and compressional speeds, respectively. The seabed will be considered as an isotropic, horizontally stratified solid, where the density $\rho$ and Lamé parameters $\mu = \rho c_t^2$ and $\lambda = \rho(c_l^2 - 2c_t^2)$ depend only on the vertical coordinate $z$. The shear modulus is small in soft sediments: $\mu \ll \lambda$. Soft sediments are alternatively referred to as almost incompressible solids because the same condition, $\mu \ll \lambda$, can be met when $\mu$ is fixed and $\lambda$ is very large.

Phase speeds $V_n$ of acoustic normal modes are comparable to the sound speed $c_w$ in water and compressional speeds in the seabed and are large compared to the shear speeds. Hence, the modal wavenumber $\xi_n = \omega/V_n$ is small compared to the wavenumber $k_t = \omega/c_t$ of shear waves. Shear waves propagate almost vertically in the seabed, making the angle $\theta_t = \arcsin(\xi_n/k_t)$ with the $z$ coordinate axis. The angle $\theta_t$ is of the first order in the dimensionless small parameter $\varepsilon$ defined as the ratio of typical values of $c_t$ and $c_l$. Only vertically polarized, or $SV$, shear waves are coupled to acoustic waves in layered media.[3] Shear waves are transverse, and therefore the ratio of vertical and horizontal components of particle displacement $u_3/(u_1^2 + u_2^2)^{1/2} = O(\varepsilon)$ in $SV$ waves.

Consider coupling of compressional, or $P$, and $SV$ waves at an interface of two homogeneous solids. Within each solid, the $P$ and $SV$ waves are described in terms of the scalar, $\varphi$, and vector, $\boldsymbol{\psi}$, potentials, respectively. Particle displacement $\mathbf{u}$ equals $\mathbf{u} = \nabla\varphi + \nabla\times\psi$. The dependence $\exp(i\xi x - i\omega t)$ of the wave field on the horizontal coordinates $x$, $y$ and time $t$ will be assumed and suppressed. Then the particle displacement in $P$–$SV$ waves has no $y$-component: $\mathbf{u} = (u_1, 0, u_3)$, and the only non-zero component of the vector potential is along the $y$ axis: $\boldsymbol{\psi} = (0, \psi, 0)$.[3]

Reflection, transmission, and conversion coefficients of plane waves at a solid-solid interface are rather cumbersome and can be found in various forms in many publications. We work with the thoroughly tested equations presented in Ref. 3. Let us introduce five axillary quantities $D_0, D_1, \ldots, D_4$:

$$\begin{aligned}
D_1 &= n^2 - m + \frac{mn^2k_t^2}{2\xi^2},\\
D_2 &= \frac{\xi}{\beta}\left[n^2 - m + \frac{(m-1)n^2k_t^2}{2\xi^2}\right],\\
D_3 &= \frac{\sqrt{n^2k_t^2 - \xi^2}}{\xi}(n^2 - m),\\
D_4 &= \frac{\sqrt{n^2k_t^2 - \xi^2}}{\beta}\left[n^2 - m - \frac{n^2k_t^2}{2\xi^2}\right],\\
D_0 &= D_1^2 + \frac{\beta}{\alpha}D_2^2 + \frac{\alpha_1}{\sqrt{n^2k_t^2 - \xi^2}}\left(D_3^2 + \frac{\beta}{\alpha}D_4^2\right)\\
&\quad + m\left(\frac{\alpha_1}{\alpha} + \frac{\sqrt{n^2k_t^2 - \xi^2}}{\beta}\right)\frac{n^4k_t^4}{4\xi^4}.
\end{aligned} \tag{10}$$

Here, $m$ and $n$ are the ratios, respectively, of densities and shear-wave wave numbers below and above the interface [Fig. 1(a)]; $\alpha = (\omega^2/c_l^2 - \xi^2)^{1/2}$ and $\alpha_1 = (\omega^2/c_{l1}^2 - \xi^2)^{1/2}$ are the vertical components of the $P$ wave wave vector above and below the interface; $\beta$ is the vertical component of the $S$ wave wave vector above the interface. The branch of the square roots is chosen in such a way that $\alpha$, $\alpha_1$, $\beta$, and $(n^2k_t^2 - \xi^2)^{1/2}$ are either real non-negative or, when complex, have a positive imaginary part.

Let either $P$ or $SV$ plane wave be incident on the interface from above. The reflection coefficients $V_{ll}$ and $V_{tt}$ of compressional and shear waves and the transformation coefficients from incident compressional to reflected shear waves, $V_{lt}$, from incident shear to reflected compressional waves, $V_{tl}$, and from of the incident compressional wave to transmitted shear wave, $W_{lt}$, are defined as ratios of the values that respective scalar and/or vector potentials $\varphi$ and $\psi$ in reflected (or, for $W_{lt}$, transmitted) and incident waves take at the interface. These coefficients are given by the following equations:[3]

$$V_{ll} = \frac{1}{D_0}\left(D_1^2 - \frac{\beta}{\alpha}D_1^2 + \frac{\alpha_1}{\sqrt{n^2k_t^2 - \xi^2}}D_3D_4\right), \tag{11}$$

$$V_{lt} = \frac{-2}{D_0}\left(D_1D_2 + \frac{\alpha_1}{\sqrt{n^2k_t^2 - \xi^2}}D_3D_4\right),$$

$$V_{tl} = -\frac{\beta}{\alpha}V_{lt}, \tag{12}$$

$$V_{tt} = \frac{1}{D_0}\left[\frac{\alpha_1}{\sqrt{n^2k_t^2 - \xi^2}}\left(D_3^2 - \frac{\beta}{\alpha}D_4^2\right) + D_1^2 - \frac{\beta}{\alpha}D_2^2 + m\left(\frac{\alpha_1}{\alpha} - \frac{\sqrt{n^2k_t^2 - \xi^2}}{\beta}\right)\frac{n^4k_t^4}{4\xi^4}\right], \tag{13}$$

$$W_{lt} = \frac{n^2k_t^2}{\xi^2 D_0}\left(D_2 + \frac{\alpha_1}{\sqrt{n^2k_t^2 - \xi^2}}D_3\right). \tag{14}$$

Equations (11)–(14) are exact. These equations simplify in the case of soft solids. In the limit of small $\varepsilon$, we find

$$V_{ll} = \frac{m\alpha - \alpha_1}{m\alpha + \alpha_1} - \frac{2m(m-1)^2\alpha\xi^2}{(m+n)(m\alpha + \alpha_1)^2k_t} + O(\varepsilon^2), \tag{15}$$

$$V_{lt} = -\frac{2m(m-1)\alpha\xi}{(m+n)(m\alpha + \alpha_1)k_t} + O(\varepsilon^2), \tag{16}$$

$$V_{tl} = \frac{2m(m-1)\xi}{(m+n)(m\alpha + \alpha_1)} + O(\varepsilon), \tag{17}$$

$$V_{tt} = \frac{m-n}{m+n} - \frac{2m(m-1)^2\xi^2}{(m+n)(m\alpha + \alpha_1)k_t} + O(\varepsilon^2), \tag{18}$$

and

$$W_{lt} = -\frac{2(m-1)\alpha\xi}{(m+n)(m\alpha + \alpha_1)k_t} + O(\varepsilon^2). \tag{19}$$

As expected, $V_{lt}$ and $W_{lt}$ vanish and $V_{ll}$ reduces to plane wave reflection coefficient at a fluid-fluid interface, when $c_t \to 0$; see Eqs. (15), (16), and (19). Equations (16) and (19) show that reflection of a $P$ wave with unit amplitude creates $SV$ waves with potential $\psi = O(\varepsilon)$ above and below the interface, when the density ratio $m \neq 1$. In contrast, reflection of an $SV$ wave with unit amplitude creates reflected $P$ and $SV$ waves with $O(1)$ potentials according to Eqs. (17) and (18). When $m = 1$, the dominant term in Eq. (17) and all linear terms in the shear speed $c_t = \omega/k_t$ vanish in Eqs. (15), (16), (18), and (19), and coupling between $P$ and $SV$ waves becomes much weaker.

Linear dependence of the magnitude of the shear-wave reflection coefficient $V_{tt}$, Eq. (13), and other reflection and transmission coefficients at solid-solid interface on $c_t$ was previously reported[36] in the related problem where $0 \le c_t/cl \ll 1$ but the ratio $c_{t1}/c_{l1}$ is not small.

In the case of a plane sound wave reflection from a fluid-solid interface, weak shear rigidity results in the second-order corrections, $O(\varepsilon^2)$, in the reflection coefficient; the transmission coefficient $W_{lt} = O(\varepsilon^2)$.[3,37] When compressional waves in the solid are evanescent ($\mathrm{Re}\alpha_1 = 0$), shear-induced changes in the absolute value and phase of the reflection coefficient are, respectively, $O(\varepsilon^3)$ and $O(\varepsilon^2)$.[3,37] Note that the effect of weak shear rigidity on wave reflection and transmission is generally much stronger at the solid-solid interface with $m \neq 1$ than at the fluid-solid interface or solid-solid interface without density contrast.

### C. Leading-order shear-induced perturbation of the wave field in a layer

In the solid layer $0 < z < h$, the vertical dependence of the scalar and vector potentials is given by

$$\varphi = \varphi_1 e^{i\alpha z} + \varphi_2 e^{-i\alpha z}, \ \psi = \psi_1 e^{i\beta z} + \psi_2 e^{-i\beta z}, \tag{20}$$

where $\varphi_2$, $\varphi_1$ and $\psi_2$, $\psi_1$ are complex amplitudes of the up- and down-propagating plane $P$ and $SV$ waves, respectively. The scalar potential $\varphi$ is non-zero, when $\mu = 0$, and is slightly perturbed by weak shear rigidity. Since $\beta = O(\varepsilon^{-1})$, the vector potential should be small, $\psi = O(\varepsilon)$, for the component $u_1 = i\xi\varphi - \partial\psi/\partial z$ of the particle displacement to remain bounded at $\varepsilon \to 0$.

In terms of the potentials, for the vertical displacement and two components of the stress tensor $\sigma_{js}$ at $z = 0$, we have[3]

$$u_3 = i\alpha(\varphi_1 - \varphi_2) + i\xi(\psi_1 + \psi_2), \tag{21}$$

$$\sigma_{13} = \mu\left[\left(k_t^2 - 2\xi^2\right)(\psi_1 + \psi_2) - 2\xi\alpha(\varphi_1 - \varphi_2)\right], \tag{22}$$

$$\sigma_{33} = \mu\left[\left(2\xi^2 - k_t^2\right)(\varphi_1 + \varphi_2) - 2\xi\beta(\psi_1 - \psi_2)\right]. \tag{23}$$

The boundary conditions at fluid-solid interface require continuity of $u_3$ and $\sigma_{33}$ and that $\sigma_{13} = 0$. Because of the latter

https://doi.org/10.1121/10.0004999

boundary condition, the quantity in the square brackets in the right side of Eq. (22) is exactly zero and, therefore, $\psi_1 + \psi_2 = O(\varepsilon^2)$. Then Eqs. (21) and (23) give

$$Z_{in} = \frac{\sigma_{33}}{i\omega u_3}\bigg|_{z=0} = \frac{\omega\rho(\varphi_1+\varphi_2)}{\alpha(\varphi_1-\varphi_2)} + O(\varepsilon^2). \tag{24}$$

Consider now the interface $z=h$ between the solid layer and solid half-space. According to Eq. (20), we have incident compressional and shear waves with amplitudes $\varphi_1$ and $\psi_1$, respectively, and reflected waves with amplitudes $\varphi_2$ and $\psi_2$. In terms of the reflection and transformation coefficients at solid-solid interface, the amplitudes of incident and reflected waves are related by two exact equations,

$$\varphi_2 e^{-i\alpha h} = V_{ll}\varphi_1 e^{i\alpha h} + V_{tl}\psi_1 e^{i\beta h}, \tag{25}$$

$$\psi_2 e^{-i\beta h} = V_{lt}\varphi_1 e^{i\alpha h} + V_{tt}\psi_1 e^{i\beta h}. \tag{26}$$

The factors $\exp(\pm i\alpha h)$ and $\exp(\pm i\beta h)$ in Eqs. (25) and (26) account for the values that the potentials in incident and reflected waves take at the boundary $z=h$. Recalling that $\psi_2 = -\psi_1 + O(\varepsilon^2)$ and neglecting terms of the second order in $\varepsilon$, the ratio $\psi_1/\varphi_1$ is found from Eq. (26). [This ratio is $O(\varepsilon)$, and, hence, weak shear rigidity results in strong, $O(\varepsilon^0)$ perturbations in the horizontal particle displacement in the bottom. Perturbations in $u_3$ and $\sigma_{33}$ remain small according to Eqs. (21) and (23).] Then $\varphi_2/\varphi_1$ is found from Eq. (25). By substitution of $\varphi_2/\varphi_1$ into Eq. (24), we obtain the impedance of the seabed: $Z_{in} = Z_0(1+C) + O(\varepsilon^2)$, where

$$Z_0 = \frac{i\omega\rho(\alpha m - i\alpha_1\tan\alpha h)}{\alpha(\alpha m\tan\alpha h + i\alpha_1)} \tag{27}$$

coincides with the impedance of the fluid bottom,[3] and $C$ is a correction of the first order in $\varepsilon$,

$$C = \frac{-2\alpha m(m-1)^2\xi^2 k_t^{-1}/(m\cot\beta h - in)}{(\alpha^2 m^2 + \alpha_1^2)\sin 2\alpha h + 2im\alpha\alpha_1\cos 2\alpha h}. \tag{28}$$

Approximate Eqs. (15)–(18) for the reflection and transformation coefficients have been used in this derivation.

When compressional wave dissipation is negligible, $\alpha_1 = i|\alpha_1|$ in normal modes, and the fluid bottom impedance $Z_0$, Eq. (27), is purely reactive (imaginary) whether $P$ waves are propagating ($\alpha$ is real) or evanescent ($\alpha$ is purely imaginary) in the layer. The first-order correction $C$, Eq. (28), has generally non-zero real and imaginary parts and, according to Eq. (5), leads to first-order attenuation of normal modes and first-order perturbations in their phase speed. First-order perturbations in the phase speed translate into first-order perturbations in the group speed and the normal mode travel times.[33] Note that the correction $C$ vanishes, and only weaker, second- and higher-order effects of shear rigidity remain, at $m = 1$, i.e., when there is no density variation within the seabed.

When $m \neq 1$, the first-order correction $C$, Eq. (28), also vanishes at discrete frequencies such that $\sin\beta h = 0$. This is caused by destructive interference of $SV$ waves that are generated at the boundary $z=h$ with the $SV$ waves that are reflected from the solid-fluid boundary at $z = 0$. To first order in $\varepsilon$, the shear-wave reflection coefficient at the fluid-solid boundary equals –1.

Derivation of Eq. (28) is based on an analysis of waves in the layer $0 < z < h$. First-order contributions to mode attenuation and their dependence on the density variation within the seabed can also be anticipated from analysis of shear waves in the half-space $z > h$. Equation (19) shows that, due to coupling at a solid-solid interface with $m \neq 1$, compressional waves in the layer generate shear waves with the vector potential $\psi = O(\varepsilon)$ in the half-space. The shear-wave vertical power flux density,[3] i.e., the power carried to infinity by the shear waves per unit area of the interface $z=h$, is $J_3 = 0.5\omega\mathrm{Im}(\sigma_{13}^* u_1 + \sigma_{33}^* u_3) = 0.5\omega^3 m\rho(n^2k_t^2 - \xi^2)^{1/2}|\psi|^2$. The power flux density and, hence, mode attenuation are of the first order in $\varepsilon$, when $m \neq 1$ and $\psi = O(\varepsilon)$. When $m = 1$, the vector potential $\psi = O(\varepsilon^2)$. Then the power flux density $I_3$ and mode attenuation are of the third order in $\varepsilon$, as was previously found[16,27] in the case of a homogeneous solid seabed.

The above findings on the effects of weak shear rigidity of the seabed on its input impedance are confirmed and extended in Sec. II D by using a different, more formal approach to calculation of the impedance.

### D. Impedance of a layered seabed

An exact expression[3] for the input acoustic impedance of the seabed that is composed of a solid layer overlaying a solid half-space is given by the following simple but cumbersome equations:

$$Z_{in} = i\omega^{-1}E_3/E_2, \tag{29}$$

where

$$E_j = \alpha_1 M_{j2} - i\omega^2\rho m\left[\left(1 - \frac{2\xi^2}{k_t^2}\right)M_{j3} - \frac{2\alpha\xi}{k_t^2}M_{j4}\right] - q\left[\xi M_{j2} - i\omega^2\rho m\left(\frac{2\xi\beta}{k_t^2}M_{j3} - \left(1 - \frac{2\xi^2}{k_t^2}\right)M_{j4}\right)\right], \quad j = 2, 3. \tag{30}$$

Equation (30) corrects two misprints in the signs in Eq. (4.3.21) of Ref. 3. The quantities $q$ and $M_{js}$ in Eq. (30) are expressed in terms of the elements $A_{js}$ of the matrix propagator[3] $\mathbf{A}$,

$$M_{js} = A_{js} - A_{j1}A_{4s}/A_{41}, \quad j = 2, 3; \quad s = 2, 3, 4; \tag{31}$$

$$q = \frac{A_{41} - \frac{\alpha_1}{\xi}A_{42} + \frac{i\omega^2\rho m}{\xi}\left(1 - \frac{2\xi^2}{n^2k_t^2}\right)A_{43} - \frac{2i\omega^2\rho m\alpha_1}{n^2k_t^2}A_{44}}{-\sqrt{n^2k_t^2 - \xi^2}\frac{A_{41}}{\xi} - A_{42} + \frac{2i\omega^2\rho m}{n^2k_t^2}\sqrt{n^2k_t^2 - \xi^2}A_{43} + \frac{i\omega^2\rho m}{\xi}\left(1 - \frac{2\xi^2}{n^2k_t^2}\right)A_{44}}. \tag{32}$$

The matrix propagator is a $4 \times 4$ matrix, which expresses the values of $u_1$, $u_3$, $\sigma_{33}$, and $\sigma_{13}$ at $z = h$ in terms of the values that these characteristics of the wave field take at $z = +0$. For a homogeneous solid layer,

$$\mathbf{A} = \mathbf{L} \cdot \mathbf{diag}\left[e^{i\alpha h},\ e^{-i\alpha h},\ e^{i\beta h},\ e^{-i\beta h}\right] \cdot \mathbf{L}^{-1}, \tag{33}$$

where **diag**[·] stands for a diagonal matrix, and

$$\mathbf{L} = \begin{pmatrix} i\xi & i\xi & -i\beta & i\beta \\ i\alpha & -i\alpha & i\xi & i\xi \\ \left(2\xi^2k_t^{-2} - 1\right)\rho\omega^2 & \left(2\xi^2k_t^{-2} - 1\right)\rho\omega^2 & -2\beta\xi k_t^{-2}\rho\omega^2 & 2\beta\xi k_t^{-2}\rho\omega^2 \\ -2\alpha\xi k_t^{-2}\rho\omega^2 & 2\alpha\xi k_t^{-2}\rho\omega^2 & \left(1 - 2\xi^2k_t^{-2}\right)\rho\omega^2 & \left(1 - 2\xi^2k_t^{-2}\right)\rho\omega^2 \end{pmatrix}. \tag{34}$$

Explicit expressions for $A_{js}$ can be found in Ref. 3.

When $h \to 0$, the matrix propagator Eq. (33) differs from the identity matrix by small terms $O(h)$, and Eqs. (29)–(34) give $Z_{in} = Z_S + O(h)$, where

$$Z_S = \frac{\omega m\rho}{\alpha_1}\left[1 - \frac{4\xi^2}{n^4k_t^4}\left(n^2k_t^2 - \xi^2 - \alpha_1\sqrt{n^2k_t^2 - \xi^2}\right)\right]. \tag{35}$$

Inspection shows that $Z_S$ coincides with the input acoustic impedance[3] of the solid half-space with density $\rho_1 = m\rho$ and the speeds $c_{t1} = c_t/n$ and $c_{l1}$ of shear and compressional waves.

Equations (29)–(34) are exact. However, the physical properties of the input impedance of the seabed with weak shear rigidity are obscured by the algebraic complexity of the equations. In addition, the matrix propagator Eq. (33) contains $\sin\beta h$ and $\cos\beta h$, which do not have limits at $c_t \to 0$ in the absence of dissipation.

By fixing $n$, $\sin\beta h$, and $\cos\beta h$ and developing the other terms in powers of ${k_t}^{-1}$, we find $Z_{in} = Z_0 + \delta Z_{in}$, where $Z_0$ is given by Eq. (27) and $\delta Z_{in} \to 0$ when $\varepsilon \to 0$. As expected, $Z_0$ coincides with the input impedance of the fluid seabed,[3] where $c_t = c_{t1} = 0$. In the absence of dissipation, $\rho$ and $\alpha^2$ are real-valued, and $\alpha_1 = i|\alpha_1|$ for propagating normal modes. Then the right side of Eq. (27) is purely imaginary whether the compressional waves are propagating ($\alpha$ is real) or inhomogeneous ($\alpha$ is imaginary) in the sediment layer $0 < z < h$.

When $m \neq 1$,

$$\delta Z_{in} = \frac{\rho c_t m(m-1)^2\xi^2\tan\beta h}{(\alpha m\sin\alpha h + i\alpha_1\cos\alpha h)^2(im + n\tan\beta h)} + O(\varepsilon^2). \tag{36}$$

Equation (36) and Eqs. (40) and (41) below have been derived from the exact Eq. (29) by using the symbolic computation capability of MATHEMATICA.[38] The magnitude of the dominant term, Eq. (36), of the impedance correction depends on the layer thickness $h$ via $\cos\alpha h$, $\sin\alpha h$, and $\tan\beta h$ because of reflections at $z = 0$ and $z = h$ and interference of compressional and shear waves in the layer. It follows from Eqs. (27) and (36) that, in the absence of dissipation,

$$\mathrm{Re}Z_{in} = \frac{\rho c_t nm(m-1)^2\xi^2\tan^2\beta h}{|\alpha m\sin\alpha h + i\alpha_1\cos\alpha h|^2(m^2 + n^2\tan^2\beta h)} + O(\varepsilon^2), \tag{37}$$

when $\alpha_1 = i|\alpha_1|$ and compressional waves are evanescent at $z > h$. The real part of the impedance is non-negative. Hence, the vertical component of the time-averaged acoustic power flux[3] $J_3 = 0.5\mathrm{Re}(pv_3^*) = 0.5|v_3^2|\mathrm{Re}Z_{in}$ at $z = 0$ is positive. As expected, acoustic energy always flows into the seabed, regardless of the conditions of interference of compressional and shear waves in the layer $0 < z < h$.

When shear wavelength is small compared to the sediment layer thickness $h$, $\tan\beta h$ rapidly oscillates with frequency. Neglecting changes of the other, gradually varying quantities in the right side of Eq. (37) over a single period of rapid oscillations and using the elementary integral

$$\int_0^\pi \frac{n\tan^2\Phi\, d\Phi}{m^2 + n^2\tan^2\Phi} = \frac{\pi}{m+n}, \tag{38}$$

where $m > 0$ and $n > 0$, we obtain

https://doi.org/10.1121/10.0004999

$$\langle \mathrm{Re}Z_{in}\rangle = \frac{\rho c_t m(m-1)^2\xi^2}{|\alpha m \sin\alpha h + i\alpha_1 \cos\alpha h|^2 (m+n)} + O(\varepsilon^2) \quad (39)$$

for the average over the narrow frequency band equal to the period of rapid oscillations. Note that, despite the factor $n$ in the numerator in the right side of Eq. (37), the average of $\mathrm{Re}Z_{in}$ does not vanish in the limit $n \to +0$ because of the singularity of the integrand in Eq. (38) at $\Phi = \pi/2$.

When $m = 1$, there is no density variation in the seabed. Then

$$\delta Z_{in} = \frac{2\rho c_t^2 \xi^2 \left[2\alpha\alpha_1(n^{-2} - 1 + \cos 2\alpha h) - i(\alpha^2 + \alpha_1^2)\sin 2\alpha h\right]}{\omega\alpha(\alpha \sin\alpha h + i\alpha_1 \cos\alpha h)^2} + O(\varepsilon^3). \quad (40)$$

Note that, to the accuracy of Eq. (40), impedance correction is independent of $n$ and the phase advance $\beta h$ of shear waves in the layer. There are no first-order terms in $\varepsilon$ in the right side of Eq. (40). In the absence of dissipation, the second-order term is purely imaginary for propagating normal modes, whether $\alpha$ is real or purely imaginary. Hence, the correction to the real part of the impedance is $O(\varepsilon^3)$, while the correction to the imaginary part of the impedance is of the second order in $\varepsilon$.

For comparison, when there are no interfaces within the seabed ($n = m = 1$, $\alpha = \alpha_1$), and the seabed is a homogeneous, almost incompressible solid half-space, we obtain

$$Z_{in} = \omega\rho\left(\frac{1}{\alpha} - \frac{4\xi^2}{\alpha k_t^2} + \frac{4\xi^2}{k_t^3}\right) + O(\varepsilon^4) \quad (41)$$

from Eq. (35). Then, for propagating normal modes, corrections due to shear rigidity to $\mathrm{Im}Z_{in}$ and, hence, to modal phase speeds are of the second order in $\varepsilon$, while corrections to $\mathrm{Re}Z_{in}$ and mode attenuation are of the third order. Equation (40) is consistent with Eq. (41). Equations (40) and (41) confirm the finding of Sec. II C that first-order perturbations in the scalar and vector potentials and in the input impedance arise from compressional-to-shear wave conversion only when there is a density change across a solid-solid interface.

## III. RESULTS

This section illustrates predictions of the theory developed in Secs. II B–II D. Figure 1(b) compares impedances of a fluid and a soft solid seabed with the same layer thickness, layer and sub-bottom densities, and compressional speeds and negligible dissipation. The impedances are given by Eqs. (27) and (29), respectively. In Figs. 1 and 2, the impedances are normalized by the absolute value of the frequency-independent impedance of the fluid half-space with compressional speed and density of the sub-bottom. This normalization does not distort the frequency dependence of the plotted quantities, renders the normalized impedance dimensionless, and simplifies comparison of the perturbations to a representative value of the magnitude of the unperturbed impedance. Impedance of the fluid bottom is purely imaginary, i.e., reactive, and gradually varies with frequency due to interference of compressional waves caused by their reflection at $z = h$ [Fig. 1(b)]. Shear rigidity adds a non-negative real, i.e., active, component of the impedance. It represents the energy that is continuously removed from the acoustic field and carried to $z \to \infty$ by shear waves. The real and imaginary parts of the impedance of the solid seabed oscillate rapidly with frequency in a quasi-periodic manner [Fig. 1(b)] due to interference of *SV* waves, to first approximation, the *SV* waves that are generated at $z = h$ and reflected at $z = 0$. The quasi-period of the frequency dependence of the impedance is close to $\Delta f = c_t/2h$ and is very small in soft sediments. Narrow frequency bands are chosen in Fig. 1(b) and other figures to reveal these rapid oscillations.

Figures 1(c) and 1(d) compare the exact calculations to the first-order perturbation theory, Eq. (36). The perturbation theory correctly reproduces qualitative details of the frequency dependence and is rather accurate quantitatively, when shear speeds are small. As the shear speed increases and reaches $c_{t1} = 400$ m/s in the sub-bottom, discrepancies between the exact and first-order calculations become significant, especially for $\mathrm{Im}Z_{in}$ [Figs. 1(c) and 1(d)], because the second- and higher-order terms in $\varepsilon$ are no longer negligible. Figures 1(c) and 1(d) show a near-linear dependence of the perturbations of the active and reactive components of the impedance on shear speed in a seabed with density stratification. Dependence of the real part of the seafloor impedance and, hence, of mode attenuation on the seabed parameters is illustrated in more detail in Fig. 2.

Using exact Eq. (29), Figs. 2(a)–2(c) compare the active component of the seafloor impedance in three scenarios, which differ only by the contrast in the shear speeds and density across the interface $z = h$. Common impedance normalization is applied in all the scenarios. It uses the sub-bottom parameters from scenario (c), which is illustrated in Fig. 2(c). In Fig. 2(a), the shear speed and density in the sub-bottom are the same as in the sediment layer. In this case, $\mathrm{Re}Z_{in}$ is frequency-independent and is proportional to $c_t^3$. This is the same behavior as predicted by Eq. (41) for homogeneous solid seabed, where *P–SV* coupling occurs only at the seafloor $z = 0$. The similarity stems from the fact that *P* and *SV* waves propagate without coupling in stratified solids with constant density and shear rigidity, regardless of compressional speed variation.[39]

Density of the seabed is constant, but there is a shear speed jump across the interface $z = h$ in scenario (b). In contrast to Fig. 2(a), Fig. 2(b) demonstrates rapid oscillations of the active component of the impedance with frequency. This is a result of interference of shear waves generated and reflected at $z = 0$ and $z = h$. Quasi-period of the $\mathrm{Re}Z_{in}$ oscillations in Fig. 2(b) increases with $c_t$, as expected. The magnitude of the active component of the impedance remains proportional to $c_t^3$, as in Fig. 2(a), but is considerably larger than in scenario (a), even after averaging over frequency.

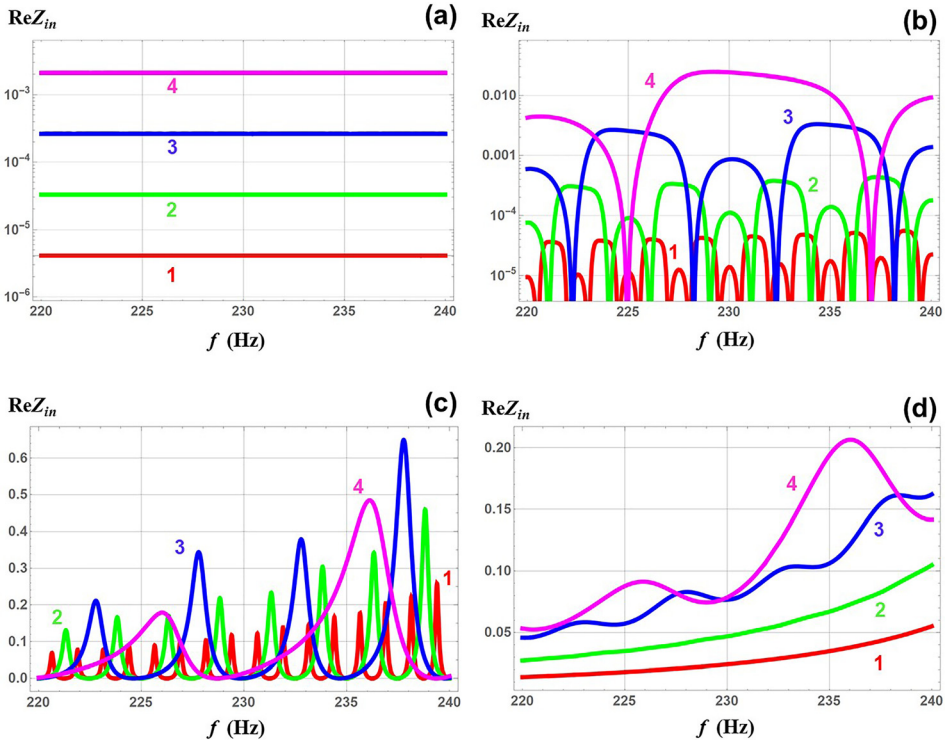


FIG. 2. (Color online) Active component of the acoustic impedance of a two-layer solid bottom with weak shear. (a) Real part of the normalized impedance is shown as a function of frequency for four values of the shear speed in the top layer: $c_t = 25$ m/s (1), 50 m/s (2), 100 m/s (3), and 200 m/s (4), when there is neither density nor shear speed variation with depth ($n = 1$, $m = 1$). The other geoacoustic parameters, $c_l$, $c_{l1}$, and $h$, and the impedance normalization are the same as in Fig. 1. (b) Same as in (a) but with different shear speeds above and below the interface $z = h$; $n = 0.5$. (c) Same as in (a) but with different shear speeds and densities above and below the interface $z = h$; $n = 0.5$, $m = 2$. (d) Same as in (c) but including the effect of shear-wave dissipation. The shear-wave absorption coefficient is 0.55 dB/$\lambda$.

The increase in Re$Z_{in}$ in scenario (b) can be attributed to shear-wave generation by $P$ waves at an additional interface and to increase in the sub-bottom shear speed compared to scenario (a).

Scenario (c) [Fig. 2(c)] represents a generic situation where there are significant changes in both density and shear speed across an interface in the seabed. Shear-wave interference and Re$Z_{in}$ oscillations with frequency of the same nature as in scenario (b) are evident in Fig. 2(c). The shape of Re$Z_{in}$ peaks in Fig. 2(c) differs from those in Fig. 2(b) because, as discussed in Sec. II C, $P$-$SV$ coupling at the boundary $z = h$ dominates when $m \neq 1$. The most significant distinction of the results in scenario (c) from those in scenarios (a) and (b) is that Re$Z_{in}$ (and, hence, the shear-wave contribution to normal mode attenuation) is *orders of magnitude* larger than in the absence of density stratification within the solid seabed [cf. Fig. 2(c) to Figs. 2(a) and 2(b)]. In Fig. 2(c), relative changes of the impedance due to shear exceed 0.6 when the shear speeds $c_l = 100$ m/s and $c_1 = 200$ m/s remain relatively small. When $c_1 \leq 200$ m/s, the magnitude of Re$Z_{in}$ in Fig. 2(c) tends to vary linearly with the shear speeds, in agreement with the theory in Secs. II C and II D. An important corollary of the linear dependence, as opposed to the cubic one in Figs. 2(a) and 2(b), is that the seafloor impedance is predicted to have a non-negligible active component even for very soft sediments [see, e.g., 0.1–0.2 peak values of the normalized active impedance in Fig. 2(c) for $c_l = 25$ m/s].

We have so far disregarded wave energy dissipation in Sec. III. A viscoelastic seabed can be treated by attributing imaginary parts to Lamé parameters or, equivalently, by replacing compressional and shear speeds with complex quantities $c_l(1 - i/Q_l)$, $c_t(1 - i/Q_t)$, and so forth.[3,40] Here, $c_l$, $c_t$, $Q_l$, and $Q_t$ are real and positive. $Q_l$ and $Q_t$ have the meaning of the quality factors for compressional and shear waves, respectively; usually $Q_l > Q_t \gg 1$.[6,40] In homogeneous viscoelastic solids, the quality factor is related to the attenuation coefficient $a$ of the respective wave in dB per wavelength by $a = 20\pi Q^{-1}/\ln 10 \approx 27.3Q^{-1}$. In soft sediments, attenuation of shear waves is much larger than attenuation of compressional waves over the same path because of the much shorter wavelength of the shear waves.

Figure 2(d) illustrates the effect of dissipation on the active component of the seafloor impedance in the generic model of two-layer soft solid seabed. In this scenario (d), the shear-wave quality factor $Q_t = Q_{t1} = 50$, and dissipation of $P$ waves is negligible. The ratio $n = c_t(1 - i/Q_t)/c_{t1}(1 - i/Q_{t1})$ remains real. Aside from the shear dissipation, all other parameters are the same in scenarios (c) and (d). To interpret the results shown in Fig. 2(d), we note first that $\tan\beta h \to i$ when $\mathrm{Im}(\beta h) \gg 1$, i.e., when shear waves are strongly attenuated within the top sediment layer. Substitution of $i$ for $\tan\beta h$ in Eq. (36) gives

$$\delta Z_{in} = \frac{\rho c_t m(m-1)^2\xi^2}{|\alpha m \sin\alpha h + i\alpha_1 \cos\alpha h|^2(m+n)} + O(\varepsilon^2). \quad (42)$$

According to Eq. (42), the shear-induced perturbation of the acoustic impedance of the seafloor is purely real and coincides with the narrowband frequency average in the absence of dissipation, Eq. (39). When shear waves are strongly attenuated while crossing the layer $0 < z < h$, $SV$ waves generated by $P$ waves at the interface $z = h$ do not reach the interface $z = 0$, and there is no interference with $SV$ waves

https://doi.org/10.1121/10.0004999

reflected from the sediment-water interface. By removing the interference, shear-wave attenuation acts just like frequency averaging and produces smooth frequency dependence of the active component of the impedance, when shear speeds are very small, such as $c_t = 25$ m/s and $c_t = 50$ m/s in Fig. 2(d). At larger shear speeds, Im($\beta h$) decreases. Then shear-wave dissipation smoothens but does not eliminate the oscillations [cf. the plots for $c_t = 100$ m/s and $c_t = 200$ m/s in Figs. 2(c) and 2(d)]. With oscillations of the active component of the impedance with frequency smoothed, Fig. 2(d) clearly shows the linear dependence of Re$Z_{in}$ on the shear speed at $c_{t1} \leq 200$ m/s, which was also pointed out in scenario (c).

In Fig. 3, we compare normal mode attenuation over soft solid seabed and a homogeneous fluid bottom with the same density and compressional wave speed as in the solid sub-bottom. $P$ wave absorption is assumed to be negligible in the solid seabed; the shear-wave quality factors $Q_t = Q_{t1} = 50$ are the same in the top sediment layer and the sub-bottom. In Fig. 3, the sound attenuation coefficient in the fluid bottom is found by equating the real parts of the input impedances of the solid seabed, Eq. (29), and the fluid bottom, $Z_{in} = \omega\rho_1/\alpha_1$. Essentially the same results (not shown) are obtained by equating the real parts of the input admittances of the bottom in the solid and fluid models. Thus, Fig. 3 shows how the loss of acoustic energy due to $P$ to $SV$ wave conversion in a soft solid seabed would be interpreted as an apparent sound absorption within the fluid bottom model. As long as attenuation per wavelength remains small, the effects on the seafloor impedance of the $P$–$SV$ wave conversion and $P$ wave dissipation are additive, and Fig. 3 also represents the difference between the apparent and true (intrinsic) $P$ wave attenuation coefficients in the bottom. Results shown in Fig. 3 depend on the wave frequency and sediment layer thickness only through the combination $fh$. Frequency values in the figure and cited below refer to $h = 10$ m and can be easily re-scaled to other $h$ values.

The frequency dependence of the apparent sound attenuation in a stratified solid bottom is characterized by fast oscillations superimposed on a decreasing trend [Figs. 3(a) and 3(b)] if there is shear speed and/or density variation within the solid seabed. The fast oscillations are due to shear-wave interference, as evidenced by the magnitude of their period and variation of the period with shear speed. These oscillations are of the same kind as seen in Figs. 1(c) and 2(b)–2(d). The oscillations are suppressed by the shear-wave dissipation at higher frequencies and at very small shear speeds [Figs. 3(a) and 3(b)]; there are no oscillations when only compressional speed varies across the interface $z = h$ [Fig. 3(c)]. Rapid oscillations of the apparent attenuation with frequency are significant, because these increase sensitivity of the attenuation modeling to uncertainty in the geoacoustic parameters, limit reproducibility of narrowband measurements, and hinder retrieval of the frequency dependence of the intrinsic $P$ wave absorption from sound attenuation measurements.

The overall trend of the apparent dissipation with frequency is qualitatively similar in Figs. 3(a)–3(c). Quantitatively, the least variation in the attenuation between frequencies below 50 Hz and above 500 Hz is observed when there is no $P$–$SV$ coupling at $z = h$ [Fig. 3(c)], and by far the largest variation occurs in the stratified seabed with a

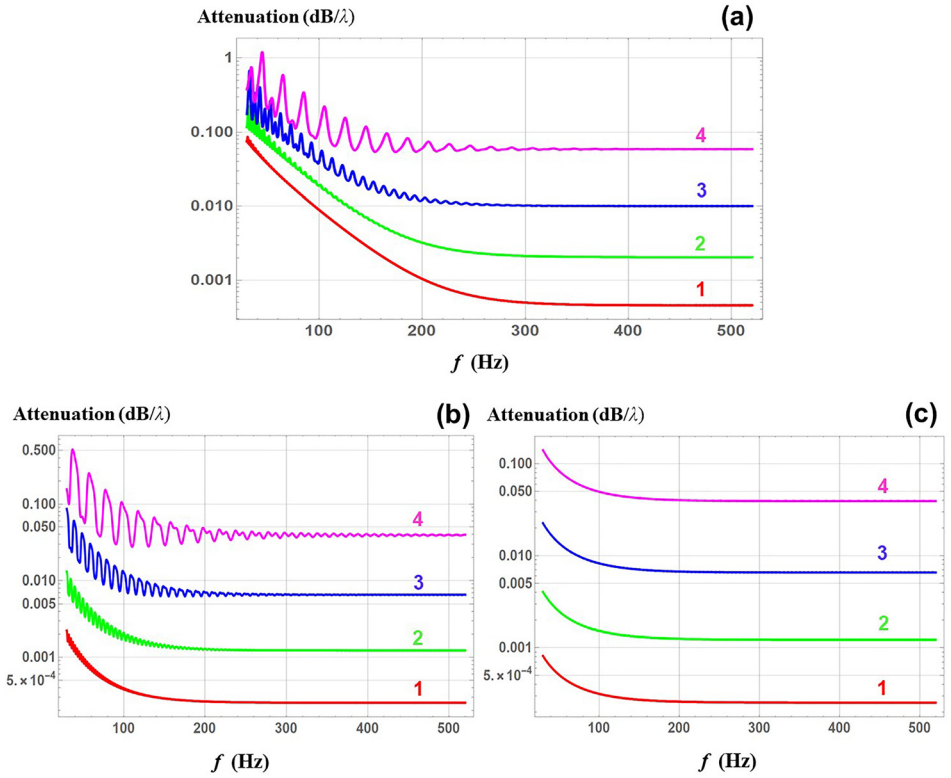


FIG. 3. (Color online) Apparent attenuation coefficient of compressional waves due to weak shear rigidity. (a) The attenuation coefficient of compressional waves in fluid bottom producing the same active component of the acoustic impedance of the seafloor as a solid seabed is shown as a function of frequency for four values of the shear speed in the top layer: $c_t = 25$ m/s (1), 50 m/s (2), 100 m/s (3), and 200 m/s (4). The layer thickness $h = 10$ m. The ratio of densities in the half-space and in the layer is $m = 2$; the ratio of shear speeds in the layer and the half-space is $n = 0.5$. Compressional wave speeds are $c_l = 1700$ m/s in the layer and $c_{l1} = 1900$ m/s in the half-space. Normal mode phase speed is 1600 m/s. The shear-wave absorption coefficient is 0.55 dB/$\lambda$. The fluid bottom is a homogeneous half-space with the same density and compressional wave speed as in the solid half-space. (b) Same as in (a) but without density stratification in the solid seabed ($m = 1$). (c) Same as in (a) but in the absence of density and shear speed density stratification in the solid seabed ($m = 1$, $n = 1$).

density contrast between the top sediment layer and the sub-bottom [Fig. 3(a)]. In the examples presented in Fig. 3, mode phase speed is smaller than $c_l$, and $P$ waves are inhomogeneous (evanescent) in the layer $0 < z < h$. Combined with the shear-wave dissipation, attenuation of $P$ waves in the layer contributes to the decrease in the effect of the interface $z = h$ on the seafloor impedance and the results in Figs. 3(a)–3(c) becoming increasingly similar at frequencies above about 300 Hz.

The magnitude of the apparent $P$ wave attenuation coefficient increases with the shear speed [Figs. 3(a)–3(c)] and reaches extremely high values at frequencies below about 125 Hz, when $c_t = 200$ m/s and there is a density contrast across the interface $z = h$ [Fig. 3(a)]. (The frequency range of very large attenuation would extend to 2.5 kHz instead of 125 Hz if the layer thickness were 0.5 m.) As expected, weaker coupling at the interface without density contrast decreases the apparent attenuation and shrinks the frequency range, where it is significant [Fig. 3(b)]. In contrast to Figs. 3(a) and 3(b), the previously considered[16,27] mechanism of $P$–$SV$ coupling at the seafloor $z = 0$ gives only marginal contributions to sound attenuation for the geoacoustic parameters considered.

## IV. DISCUSSION

Weak shear rigidity of the seabed results in attenuation and variations of the phase and group speeds of acoustic normal modes of the underwater waveguide. The effects of weak shear rigidity on acoustic normal modes, which have phase and group speeds on the order of the sound speed in water and $P$ waves in the bottom, are generally small (but not negligible), as discussed in Secs. II and III. The full set of normal modes in a waveguide with solid bottom also includes Scholte wave(s), or "slow" interface waves, the phase and group speeds of which are on the order of the shear speed; see Refs. 3, 37, 39, 41, and 42 and references therein. Unlike the acoustic modes considered in this paper, the weak shear rigidity and its variation with depth are the dominant factors, rather than a perturbation, for the "slow" interface waves.

It is often implied[5,28] that the difference between the wavenumbers of the acoustic normal modes in waveguides with a fluid bottom and a solid bottom with weak shear rigidity can be readily described by a perturbation theory. To our knowledge, no such perturbation theory is available for an arbitrary stratified seabed. Perturbation theory[30–32] for normal modes in arbitrary stratified solid and fluid-solid waveguides predicts a linear dependence of the mode wavenumbers perturbations on small changes in the density and the elastic moduli, such as the Lamé parameters. As in fluid waveguides,[33] the mode wavenumber perturbation is given by an integral of weighted environmental perturbations over depth, with the weights (sensitivity kernels) expressed in terms of the shape function of the unperturbed mode.[30–32] When the small shear modulus $\mu = \rho(z)c_t^2(z)$ in soft solid bottom is considered as a perturbation of the problem with a fluid bottom, the theories[30–32] predict the mode wavenumber perturbations to be of the second order in $c_t$, which is incorrect. It is shown by two distinct techniques in Secs. II C and II D that the mode wavenumber perturbation is, in fact, of the first order in $c_t$ when there is density stratification in the solid bottom.

Derivations of the perturbation theories[30–32] assume that small environmental perturbations necessarily result in small perturbations of the wave field in the mode. This is not the case at transition from fluid to solid bottom. As pointed out in Sec. II C, the transition from an (inviscid) fluid to solid bottom is a singular perturbation in the sense that the appearance of infinitesimal $\mu$ brings about finite, non-zero changes in particle displacements in the mode. The perturbation theories[30–32] presume regular perturbations and fail to describe the effects of weak shear rigidity, which is a singular perturbation of the fluid bottom model.

Shear waves have much shorter wavelength than compressional waves in soft solids. A sediment layer can be thin for $P$ waves ($|\alpha h| \ll 1$) and thick for SV waves ($|\beta h| \sim 1$ or $|\beta h| \gg 1$). As pointed out in Sec. II D, the effect of the top sediment layer vanishes, and only second- and higher-order effects of shear rigidity remain, when $h \to 0$. However, Eqs. (36) and (37) show that the larger, first-order shear-wave effects are present as long as $|\beta h| \sim 1$ or greater, even when $|\alpha h| \to 0$. Hence, weak shear makes acoustic normal modes sensitive to surficial bottom layers that are much thinner than acoustic wavelength. This observation has important implications for geoacoustic inversions. While a few layers with some averaged parameters may be suitable to match normal mode dispersion in a fluid bottom model, a much more detailed representation of the density and shear speed stratification in surficial sediments may be necessary to correctly reproduce mode attenuation and its frequency dependence.

In this paper, we focused on the impact of weak shear rigidity of the seabed on acoustic normal modes. The results of Secs. II and III that are expressed in terms of the input acoustic impedance of the seabed can be also readily used to investigate the effect of the slow shear waves on sound reflection from the seafloor[43] and the bottom loss at reflection in particular. Similarly, with the complex "shear speed" $c_t = (1 - i)(\omega\nu/2)^{1/2}$, where $\nu$ is kinematic viscosity of the fluid,[3] results of Secs. II and III explicitly describe the effect of viscosity on the acoustic impedance and sound reflection from a stratified viscous fluid.

## V. CONCLUSIONS

Weak shear rigidity of stratified marine sediments is found to have a much stronger effect on dispersion of bottom-interacting normal modes and especially on sound attenuation than was previously surmised based on oversimplified seabed models.[16,17,27,29] With the effects of the weak shear being larger and more intricate than previously predicted, applicability of the effective fluid bottom models and the effect of shear waves on the experimentally measured

https://doi.org/10.1121/10.0004999

frequency dependence of the sound dissipation may need to be re-assessed.

Acoustic effects of shear rigidity originate from coupling between sound and shear waves at the seafloor and within inhomogeneous seabed. Coupling between compressional and shear waves at interfaces within the bottom is shown to be far more efficient than the coupling at the water-sediment interface. In terms of the small ratio of the shear to compressional wave speeds in soft sediments, first-order contributions to mode travel time and attenuation result from the *P* and *SV* wave coupling in the seabed with density stratification. These first-order effects are generally much stronger and, because of shear-wave interference, have a more complicated frequency dependence than previously studied second-order effects on mode travel times and third-order attenuation effects in the case of homogeneous solid seabed or bottom with constant density. The acoustic effects of weak shear tend to be most pronounced at lower frequencies, with the frequency scale being controlled by the shear-wave travel time within individual sediment layers, the rate of change of the sediment properties with depth, and the shear-wave dissipation.

The primary implications of this research are for geoacoustic inversions and especially for measurements of the intrinsic (volume) dissipation of compressional and shear waves. To capture the first-order shear effects correctly, geoacoustic models must include a realistic description of density variation in the seabed in addition to compressional and shear speed profiles. A higher vertical spatial resolution than in the fluid bottom models is required, particularly for the density and shear speed.

The shear effects are much stronger in the seabed containing dissimilar surficial layers than in a seabed with averaged parameters. Our results suggest that, for narrowband signals, the shear-wave contributions to sound attenuation in the bottom can be overly sensitive to uncertain and spatially varying details of sediment stratification, making broadband and/or long-range measurements preferable. At low frequencies, shear-wave contributions to sound attenuation in stratified sediments remain significant even for very low shear speeds. Because of their non-negligible magnitude and non-monotonic frequency dependence, great care needs to be exercised in characterizing and separating the contributions to measured attenuation due to compressional-to-shear wave conversion in order to reliably evaluate the frequency dependence of the intrinsic dissipation of compressional waves.

## ACKNOWLEDGMENTS

This work was supported in part by the Ocean Acoustics program of the Office of Naval Research, Grant Nos. N00014-20WX01312 and N00014-21WX01234, and National Science Foundation Grant No. OCE1657430. The author expresses his appreciation to Dr. D.M.F. Chapman, Dr. N.R. Chapman, Dr. C.W. Holland, and Dr. G.R. Potty for stimulating discussions of the role that the shear rigidity of marine sediments plays in underwater sound propagation.

[1]J. Jarzynski, "Mechanisms of sound attenuation in materials," in *Sound and Vibration Damping with Polymers*, edited by R. D. Corsaro and L. H. Sperling (American Chemical Society, Washington, DC, 1990), pp. 167–207.
[2]F. F. Legusha, "The Konstantinov effect and sound absorption in inhomogeneous media," Sov. Phys. Usp. **27**(11), 887–895 (1984).
[3]L. M. Brekhovskikh and O. A. Godin, *Acoustics of Layered Media. 1: Plane and Quasi-Plane Waves*, 2nd ed. (Springer, Berlin, 1998), pp. 6–9, 11–19, 26–34, 87–112, 144–149.
[4]E. L. Hamilton, "Geoacoustic modeling of the sea floor," J. Acoust. Soc. Am. **68**, 1313–1340 (1980).
[5]B. Katsnelson, V. Petnikov, and J. Lynch, *Fundamentals of Shallow Water Acoustics* (Springer, New York, 2012), pp. 65–70, 157–161, 377–390.
[6]D. R. Jackson and M. D. Richardson, *High-Frequency Seafloor Acoustics* (Springer, New York, 2007).
[7]F. B. Jensen, W. A. Kuperman, M. B. Porter, and, and H. Schmidt, *Computational Ocean Acoustics*, 2nd ed. (Springer, New York, 2011).
[8]W. M. Carey, A. D. Pierce, R. E. Evans, and J. D. Holmes, "On the exponent in the power law for the attenuation at low frequencies in sandy sediments," J. Acoust. Soc. Am. **124**(5), EL271–EL277 (2008).
[9]W. A. Kuperman and F. Ingenito, "Spatial correlation of surface generated noise in a stratified ocean," J. Acoust. Soc. Am. **67**, 1988–1996 (1980).
[10]J. S. Perkins, W. A. Kuperman, F. Ingenito, L. T. Fialkowski, and J. Glattetre, "Modeling ambient noise in three-dimensional ocean environments," J. Acoust. Soc. Am. **93**(2), 739–752 (1993).
[11]A. A. Aredov and A. V. Furduev, "Angular and frequency dependencies of the bottom reflection coefficient from the anisotropic characteristics of a noise field," Acoust. Phys. **40**(2), 176–180 (1994).
[12]N. M. Carbone, G. B. Deane, and M. J. Buckingham, "Estimating the compressional and shear wave speeds of a shallow water seabed from the vertical coherence of ambient noise in the water column," J. Acoust. Soc. Am. **103**(2), 801–813 (1998).
[13]B. F. Kuryanov, "Russian investigations of ocean noise," in *History of Russian Underwater Acoustics*, edited by O. A. Godin and D. R. Palmer (World Scientific, Singapore, 2008), pp. 197–234.
[14]X. Zang, M. G. Brown, and O. A. Godin, "Waveform modeling and inversion of ambient noise cross-correlation functions in a coastal ocean environment," J. Acoust. Soc. Am. **138**(3), 1325–1333 (2015).
[15]O. A. Godin, "Acoustic noise interferometry in a time-dependent coastal ocean," J. Acoust. Soc. Am. **143**(2), 595–604 (2018).
[16]J. M. Collis, A. D. Pierce, and, and W. M. Carey, "Shear waves and the discrepancy between perceived and ideal frequency power laws for sediment attenuation," Proc. Mtgs. Acoust. **2**, 005002 (2007).
[17]A. D. Pierce and W. M. Carey, "Sediment shear as a perturbation in geoacoustic inversions and an explanation of the anomalous frequency dependence of the attenuation," Proc. Mtgs. Acoust. **8**, 005001 (2009).
[18]J. X. Zhou, X. Z. Zhang, P. H. Rogers, and J. Jarzynski, "Geoacoustic parameters in a stratified sea bottom from shallow-water acoustic propagation," J. Acoust. Soc. Am. **82**, 2068–2074 (1987).
[19]J. X. Zhou, X. Z. Zhang, and D. P. Knobles, "Low-frequency geoacoustic model for the effective properties of sandy seabottoms," J. Acoust. Soc. Am. **125**(5), 2847–2866 (2009).
[20]C. W. Holland and J. Dettmer, "*In situ* sediment dispersion estimates in the presence of discrete layers and gradients," J. Acoust. Soc. Am. **133**(1), 50–61 (2013).
[21]M. A. Biot, "Generalized theory of acoustic propagation in porous dissipative media," J. Acoust. Soc. Am. **34**, 1254–1264 (1962).
[22]R. Stoll, *Sediment Acoustics* (Springer-Verlag, New York, 1989).
[23]N. P. Chotiros and M. J. Isakson, "A broadband model of sandy ocean sediments: Biot–Stoll with contact squirt flow and shear drag," J. Acoust. Soc. Am. **116**, 2011–2022 (2004).
[24]N. P. Chotiros, "A porous medium model for mud," J. Acoust. Soc. Am. **149**(1), 629–644 (2021).
[25]M. J. Buckingham, "On pore-fluid viscosity and the wave properties of saturated granular materials including marine sediments," J. Acoust. Soc. Am. **122**(3), 1486–1501 (2007).
[26]M. J. Buckingham, "Wave speed and attenuation profiles in a stratified marine sediment: Geo-acoustic modeling of seabed layering using the viscous grain shearing theory," J. Acoust. Soc. Am. **148**(2), 962–974 (2020).

[27]A. O. Williams and R. K. Eby, "Acoustic attenuation in a liquid layer over a 'slow' viscoelastic solid," J. Acoust. Soc. Am. **34**(6), 836–843 (1962).
[28]D. D. Ellis and D. M. F. Chapman, "A simple shallow water propagation model including shear wave effects," J. Acoust. Soc. Am. **78**(6), 2087–2095 (1985).
[29]G. R. Potty and J. H. Miller, "Effect of shear on modal arrival times," IEEE J. Ocean. Eng. **45**(1), 103–115 (2019).
[30]H. Takeuchi and M. Saito, "Seismic surface waves," in *Seismology: Surface Waves and Earth Oscillations*, edited by B. A. Bolt (Academic, New York, 1972), pp. 217–295.
[31]B. A. Auld, *Acoustics Fields and Waves in Solids*, (Wiley, New York, 1973), Vol. 2, Chaps. 10 and 12.
[32]K. Aki and P. G. Richards, *Quantitative Seismology: Theory and Methods* (Freeman, San Francisco, 1980), Chap. 7.
[33]L. M. Brekhovskikh and O. A. Godin, *Acoustics of Layered Media. 2: Point Sources and Bounded Beams*, 2nd extended ed. (Springer, Berlin, 1999), pp. 150–155, 166–169, 170–177.
[34]O. A. Godin, "Acoustic-gravity waves in atmospheric and oceanic waveguides," J. Acoust. Soc. Am. **132**(2), 657–669 (2012).
[35]O. A. Godin, B. Katsnelson, and T. W. Tan, "Normal mode dispersion and time warping in the coastal ocean," J. Acoust. Soc. Am. **146**(3), EL205–EL211 (2019).
[36]B. Bianco, A. Cambiaso, and T. Tommasi, "On the boundary conditions for acoustic waves at a solid–solid or fluid–solid interface," J. Acoust. Soc. Am. **95**(1), 40–44 (1994).
[37]O. A. Godin, T. J. Deal, and H. Dong, "Physics-based characterization of soft marine sediments using vector sensors," J. Acoust. Soc. Am. **149**(1), 49–61 (2021).
[38]Wolfram Research, Inc., Mathematica (version 11.3) (Wolfram Research, Champaign, IL, 2018).
[39]W. M. Ewing, W. S. Jardetzsky, and F. Press, *Elastic Waves in Layered Media* (McGraw-Hill, New York, 1957), pp. 8–9, 124–125.
[40]J. P. Montagner and B. L. N. Kennett, "How to reconcile body-wave and normal-mode reference Earth models," Geophys. J. Int. **125**(1), 229–248 (1996).
[41]O. A. Godin and D. M. F. Chapman, "Dispersion of interface waves in sediments with power-law shear speed profiles. I: Exact and approximate analytical results," J. Acoust. Soc. Am. **110**, 1890–1907 (2001).
[42]D. M. F. Chapman and O. A. Godin, "Dispersion of interface waves in sediments with power-law shear speed profiles. II: Experimental observations and seismo-acoustic inversions," J. Acoust. Soc. Am. **110**, 1908–1916 (2001).
[43]J. Belcourt, C. W. Holland, S. E. Dosso, J. Dettmer, and J. A. Goff, "Depth-dependent geoacoustic inferences with dispersion at the New England Mud Patch via reflection coefficient inversion," IEEE J. Ocean. Eng. **45**(1), 69–91 (2020).